Resistive loss at 10 GHz in *c*-axis-aligned *in-situ*-grown $YBa_2Cu_3O_7$ films

S. S. Laderman, R. C. Taber, R. D. Jacowitz, and J. L. Moll
Hewlett Packard Company, 3500 Deer Creek Road, Palo Alto, California 94304

C. B. Eom
Department of Materials Science & Engineering, Stanford University, Stanford, California 94305

T. L. Hylton, A. F. Marshall,* T. H. Geballe, and M. R. Beasley
Department of Applied Physics, Stanford University, Stanford, California 94305
(Received 23 July 1990)

The resistive losses near 10 GHz are measured at 4.2 K for ten *c*-axis-oriented $YBa_2Cu_3O_7$ thin films deposited *in situ* on MgO substrates. The losses range from 16 ± 3 $\mu\Omega$, the lowest value reported to date for a thin film of $YBa_2Cu_3O_7$ to 740 ± 150 $\mu\Omega$, a difference of more than a factor of 40. Among the same films, the dc resistivity at 100 K ranges from 50 to 155 $\mu\Omega$ cm, about a factor of 3. We show that the losses in the higher-loss samples can be accounted for by the presence of small fractions of *c*-axis-aligned grains highly misaligned in the plane of those films. Volume fractions of highly misaligned *c*-axis-oriented grains as low as 4% lead to losses above 500 $\mu\Omega$, more than 25 times higher than the loss in the lowest-loss film reported here. Among the lower-loss films having less than 0.15 vol % highly misaligned grains, a substantial portion of the losses are due to additional mechanisms. Among these films, the losses are found to be lower in the films with lower normal-state resistivities and higher transition temperatures (T_c). For all samples, the losses increase with increasing deviations from structural or electrical behavior expected for ideal single crystals. The loss in even the lowest-loss film is orders of magnitude above that expected for an ideal isotropic BCS superconductor having the same T_c. The observed loss level is consistent with the presence of a large density of uncondensed carriers.

I. INTRODUCTION

In conventional BCS (low-T_c) superconducting materials, the surface resistance (R_s) at microwave frequencies can generally be minimized by making the sample as chemically and structurally perfect as possible.[1] The history to date of the more recently discovered superconducting (high-T_c) cuprates has shown that lower-dc resistivities, sharper superconducting transitions, shorter penetration depths, and lower microwave resistive losses result as samples are made more like ideal single crystals.[2] These changes in properties of the high-T_c samples have most often been associated with the elimination of impurity phases, more uniform oxygenation of the superconducting phase, and improved alignment of crystallites within the superconducting material.

Very recently, high-purity, highly epitaxial $YBa_2Cu_3O_7$ thin films have been routinely made *in situ* by off-axis sputtering from a stoichiometric $YBa_2Cu_3O_7$ target.[3] As indicated by their lack of appreciable impurity phases, high degree of epitaxial alignment perpendicular to their surface, low-dc normal-state resistivities, and high surface smoothness, such films more closely approximate single crystals than do typical post-deposition annealed films. However, some properties, such as their high critical currents, depressed T_c's, and expanded *c*-axis lattice parameters, are distinctly different from those of equilibrium single crystals. The properties shared with crystals suggest that these films may be significantly less granular in character than post-deposition annealed films. Since it was known that electrically weak boundaries amongst intragranular superconducting material could lead to high resistive losses at microwave frequencies,[4] the possibility of lessened granularity leads to the anticipation that such films would show lower microwave resistive losses. For this reason, the losses in a series of such films was examined.

In this report, results taken at 4.2 K are emphasized. In contrast to ideal BCS superconductors at the same reduced temperature, T/T_c, the temperature dependence of the loss for several of these samples is measured to be rather weak near 4.2 K.[5] It is also found that the absolute value of the loss at 4.2 K from the lowest-loss sample is less than that reported for any $YBa_2Cu_3O_7$ samples to date but well above the level expected for ideal isotropic BCS superconductors with the same T_c. Among the remaining samples, the losses are larger for the films with greater deviations in structural and dc electrical qualities from those associated with bulk single crystals. The experimentally deduced relationships between R_s and structural aspects of the films are described in Sec. III. The experimentally deduced relationships between R_s and some dc electrical properties are described in Sec. IV. The data are discussed in the context of a two-fluid picture and microscopic loss mechanisms in Sec. V. Conclusions of this work are summarized in Sec. VI.

II. EXPERIMENTAL PROCEDURES

$YBa_2Cu_3O_7$ films are deposited by sputtering onto 10×10 mm^2 MgO substrates using a single stoichiometric target as previously described.[3] Ten samples deposited during five independent deposition cycles are discussed here. Samples are deposited at nominal temperatures varying from 650 to 720 °C and pressures of 10 and 50 μm. The dependence of properties on the deposition conditions and their reproducibility are discussed elsewhere.[3,6] Thicknesses are varied from 300 to 500 nm. The thickness variations did not correlate to the properties discussed in this work.

The resistive losses near 10 GHz are measured in a parallel plate resonator geometry. R_s values are typically determined from resonances with frequencies in the range of 11–13 GHz. For comparison, the values reported here have been scaled to 10 GHz using an ω^2 law, where ω is the microwave frequency. The resistance in each plate of the resonator contributes to the measured loss. Values for each $YBa_2Cu_3O_7$, film are measured at 4.2 K using a Nb film as the counter plate. The measured loss of the Nb film is 18 $\mu\Omega$. The contribution of the Nb is removed assuming that the radiation and dielectric losses are negligible. In this sense, the values reported here are for the $YBa_2Cu_3O_7$ film alone. Whenever R_s is mentioned below, the value at 4.2 K scaled to 10 GHz is implied. The R_s data are always collected at rf field levels such that the observed R_s value was insensitive to the tenfold increases in the field level. Typically the rf magnetic field at the surface is below 1 Oe under these conditions.

Undoubtedly, leakage of radiation makes some contribution to the observed losses reported here. Increased penetration depths lead to larger losses both resistively and radiatively. That there is some radiative loss is confirmed by backing one of a pair of $YBa_2Cu_3O_7$-MgO pieces with a Nb film and observing a 10% decrease in measured loss when lowering the temperature from above to below the Nb T_c. No attempt is made here to separate this radiative loss from resistive losses. In this work, R_s refers to the observed loss value derived from the resonator Q as if radiation losses were entirely absent.

The details of the apparatus used to measure R_s and a more complete analysis of its operation and characteristics are described elsewhere.[7] Here, trends amongst small differences and the meaning of the absolute values of the losses are examined closely. Briefly told, experiences which justify this approach include the close correspondence of the absolute loss measured for Nb sputtered films and the absolute loss expected, the agreement between expected and observed temperature dependencies of the losses and the fractional frequency shifts for Nb films and for $YBa_2Cu_3O_7$ films are near their respective T_c's for two different dielectric spacer materials, and, the agreement between the measured loss expected and found as a function of dielectric spacer thickness. The reproducibility of numerous 4.2 K measurements of Nb films was of the order of 10% and the measurement of the dielectric spacer thickness, needed to assign an absolute scale to the observed losses, is about 10%. Nominal uncertainties for the lower-loss values reported here are therefore 20%. As the loss rises as high as 500 $\mu\Omega$ or more, additional uncertainties related to the increase in background and resonance-shape distortions raise the level of uncertainty.

The reproducibility of R_s values from individual $YBa_2Cu_3O_7$ samples is generally as good as that just quoted for Nb. Macroscopic inhomogeneities, particularly near the edges of the films, appear to lead, in some cases, to greater spreads as evidenced by differences between measurements made with identically sized $YBa_2Cu_3O_7$ or Nb counter plates and slightly undersized Nb counter plates. The numbers reported here are consistent for from two to four trials for each film. As will be seen, the conclusions of this work do not depend on the absolute value of the uncertainties in R_s. Some of the conclusions do, however, depend on the belief that 16 $\mu\Omega$ is above the resolution limit of the resonator. This belief is warranted by the data from Nb from 4.2 K and higher which imply that the sensitivity of the apparatus is 5 $\mu\Omega$.[7] Direct measurements at temperatures below 4.2 K have not yet been performed.

X-ray data are collected using Cu K_α radiation with a four-circle system described elsewhere[8] and using Cu $K_{\alpha1}$ radiation with a dedicated rocking-curve apparatus employing a perfect Ge first crystal. Rocking-curve data are reported for the $YBa_2Cu_3O_7$ (005) reflection and the MgO (002) reflection. The full widths at half maximum of the MgO (002) rocking curves are all close to 0.02°, ten times smaller than the narrowest $YBa_2Cu_3O_7$ rocking curve found here. These data reflect the perfection of the out-of-plane epitaxy as well as the degree of inhomogeneous strain in the samples. The perfection of the in-plane epitaxy was first examined semiquantitatively by exploring the sample orientation dependence of the scattered intensity with the detector fixed at the angle corresponding to the $YBa_2Cu_3O_7$ (103) d-spacing. The samples are mounted with their surface normals along the instrument ϕ axis. After centering the (103) reflection from c-axis-oriented $YBa_2Cu_3O_7$ having an [100] or [010] along the substrate [100], the instrument ϕ axis is scanned. This scan closely approximates a rotation about the $YBa_2Cu_3O_7$ [001] of c-axis-aligned grains. The intensity increases for ϕ values corresponding to more common in-plane epitaxial alignments in proportion to their volumes. For more quantitative analysis, additional x-ray data are acquired. Radial scans are performed at particular ϕ values to obtain background-corrected integrated intensities. Samples are then compared by scaling according to the strength of the principal orientation, taking into account the small observed variations in peak widths.

After measuring R_s and the x-ray data, nine of the samples were cut without solvents into four pieces using a diamond saw. Each piece is approximately 5×5 mm^2 in size. One piece from each film is patterned photolithographically using wet chemical techniques. The patterned pieces are used to determine dc resistivities as a function of temperature with a four-terminal measurement. Thicknesses are measured using a Dektak profilemeter across these patterns. Critical currents are

measured using unpatterned 5×5 mm^2 pieces and a vibrating sample magnetometer. Magnetization data are converted to critical currents using the Bean model.[9] Since many of the samples have the same critical current, it seems unlikely that the values are markedly affected by gross inhomogeneities on the scale of the original 10-mm sample size. The ac susceptibility at 10 kHz is measured as a function of temperature to determine T_c in the uncut sample. The ac measurements are found to yield results consistent with the transport data in four samples measured both ways.

III. CORRELATION OF MICROWAVE LOSS AND THE $YBa_2Cu_3O_7$ STRUCTURE

X-ray-diffraction analyses are used to quantify the quality of epitaxy, phase purity, and *c*-axis lattice parameters of the films. A summary of these attributes appears in Table I. The structural feature which clearly correlates to R_s among these samples is the volume fraction of *c*-axis-aligned $YBa_2Cu_3O_7$ misaligned at high angles in the plane of the film.

The volume fraction of misaligned *c*-axis material is determined by asymmetric diffraction analysis as described in detail in Sec. II. Figure 1(a) shows a ϕ-axis scan for a sample which contains a few percent by volume of misaligned material. Figure 1(b) shows the scan for a sample which contains much less than 1% by volume of misaligned material. In both cases, the most prominent orientation apart from $YBa_2Cu_3O_7$ [100]||MgO [100] or $YBa_2Cu_3O_7$ [010]||MgO [100], defining $\phi=0$, is one differing by 45°. Such misorientations for $YBa_2Cu_3O_7$ on MgO have recently been reported by several groups.[10–12] In the samples with larger amounts of misoriented *c*-axis material, peaks at $\phi=26.5°$, 34°, 56°, and 64° are also seen. For the most prominent alignments, the x-ray scans clearly indicate the relative prominence of the different directions. Note, though, that in the slowly varying region of the ϕ scan, radial scans sometimes reveal Bragg scattering at a very weak level. Including even this contribution, the majority of misaligned material is always found at 45°. The signal at $\phi=45°$ is used here as the estimate of *c*-axis material misaligned at high angles in the plane of the film.

Figures 2(a) and 2(b) show the relation between R_s and the quantity of such misaligned material. It is seen from Fig. 2(a) that two of the samples have roughly 25 times higher loss and roughly 25 times more misaligned material than the others, suggesting that the loss in these two samples is dominated by high-angle grain-boundary effects. These two samples indicate that the presence of as little as 4 vol % highly misaligned *c*-axis grains puts R_s over 500 $\mu\Omega$. Figure 2(b) shows the trend for the eight lower-loss samples. The lines are the same in both parts of Fig. 2. The solid trend line is a linear least-squares fit to the seven lowest-loss samples, those with misaligned fractions below 0.15 vol %. The dashed line passes through the origin and the average position of the two highest-loss samples.

From Figs. 2(a) and 2(b), three conclusions are drawn. First, a correlation with a correlation coefficient $r=0.7$ is found between R_s and the misaligned fraction among the samples with the smallest observed fractions. This suggests a measurable component of their loss is due to high-angle boundary phenomena. Second, the intercept of the empirical trend (solid line) amongst the lowest-loss samples to zero misaligned fraction is about 12 $\mu\Omega$. This shows that a substantial component of the loss in the lowest-loss sample is due to other mechanisms. Third, the extrapolation of the empirical trend (solid line) observed amongst the lowest-loss samples to the higher levels of misaligned fractions observed for the two-highest loss samples is in the vicinity of the observed losses, although this extrapolation is many times further than the data range used to define the line. This supports the interpretation of the observed range used to define the line. This supports the interpretation of the observed correlation among the lower-loss samples resulting from the remnance of high-angle boundary effects. However, the weakness of the correlation due to the high degree of scatter amongst the low-loss samples also supports the inference drawn from the zero fraction intercept that ad-

TABLE I. R_s and structural characteristics [volume percent of highly misaligned *c*-axis grains, *c* lattice parameter, (005) rocking-curve full width at half maximum, relative impurity content, apparent presence of *a*-axis-oriented grains and thickness, respectively] of the $YBa_2Cu_3O_7$ films. The thickness of the film having $R_s=26$ μQ is estimated from the deposition parameters.

R_s (10 GHz, 4.2 K) ($\mu\Omega$)	$I(45)/I(0)$ $\times100$	c_0 (Å)	$\Delta\omega$ (deg)	Impurity $I(2.62)/I(005)$ $\times100$	*a* axis	Thickness (nm)
16	0.026	11.73	0.37	0.15	no	450
23	0.129	11.74	0.80	0.84	no	420
25	0.031	11.73	0.34	0.21	no	400
26	0.093	11.71	0.31	0.38	no	(400)
38	0.122	11.71	0.27	0.00	yes	300
42	0.127	11.74	0.40	0.55	no	450
64	0.136	11.74	0.36	0.00	yes	300
108	0.225	11.75	0.34	0.00	no	500
545	3.8	11.69	0.26	0.25	no	320
744	3.5	11.76	0.45	0.00	yes	500

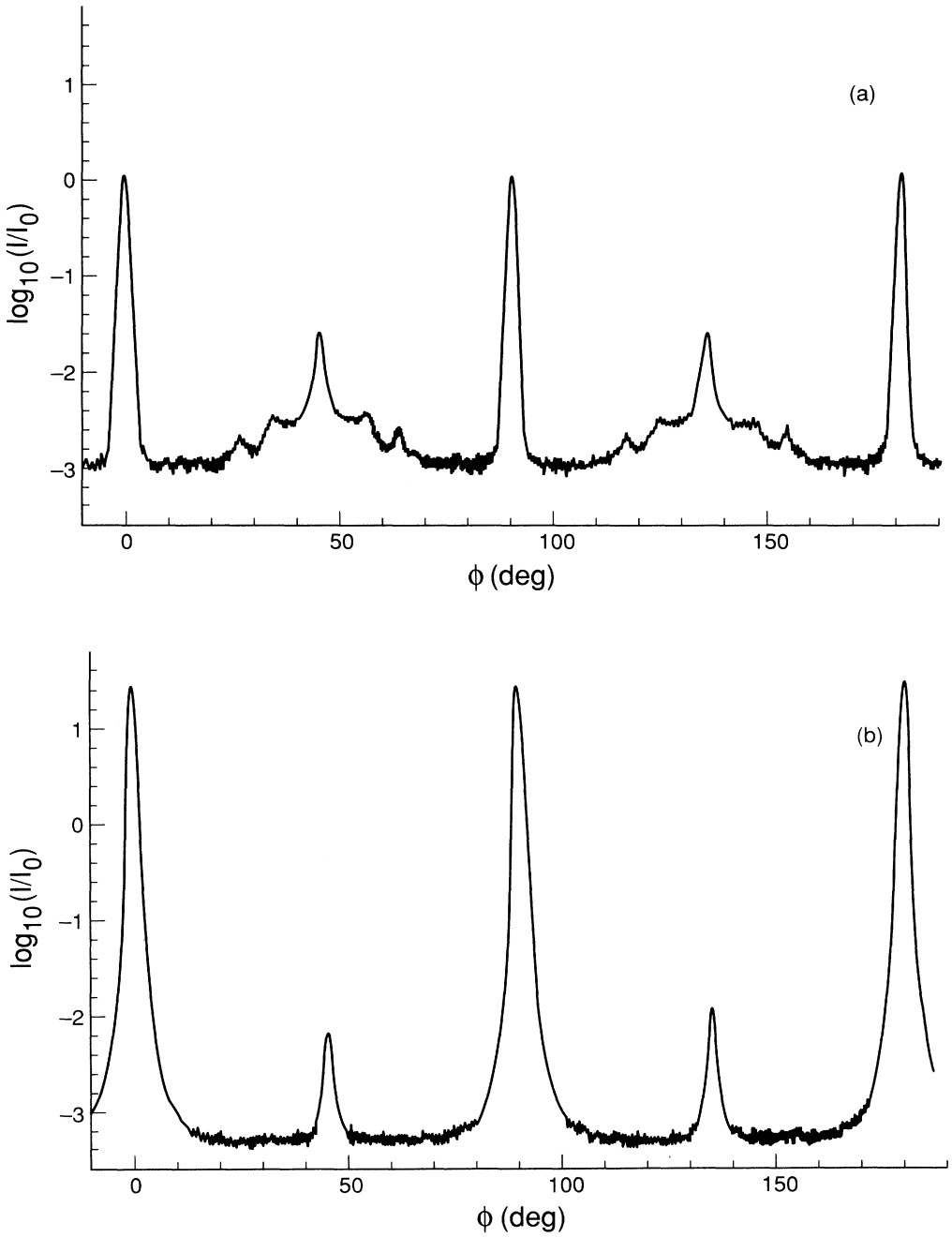

FIG. 1. X-ray diffraction from the $YBa_2Cu_3O_7$ (103) reflection during an azimuthal scan about the $YBa_2Cu_3O_7$ c axis showing highly misaligned c-axis oriented grains in (a) the sample with the highest loss and (b) the sample with the lowest loss. Note that the instrument settings determining the absolute ratio of I to I_0 at fixed sample scattering power and the background level were changed between the times the two scans were taken. These changes do not alter the volume fractions of misaligned material deduced from the data.

ditional factors separate from the volume fraction of misaligned material contribute as well. This result, that the loss in the lowest-loss sample is not dominated by a mechanism associated with the misaligned grains, is underscored with reference to the dashed line in Fig. 2(b). The observed losses sit above this line, which itself passes through the highest-loss values and the origin. If the observed losses are all dominated by the mechanisms associated with the misaligned grains, the data would be expected to follow the dashed line and extrapolate more closely to zero loss at zero misaligned fraction. Additional correlations and possible associated loss mechanisms will be further discussed in the following sections. The remainder of this section documents structural aspects of

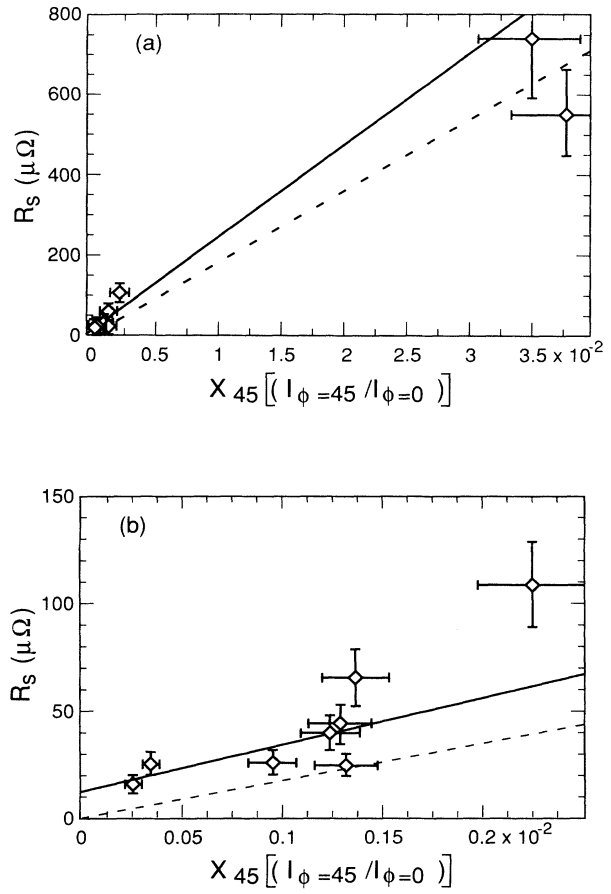

FIG. 2. R_s vs the volume percent of c axis grains misaligned at 45° in the plane for (a) all samples and (b) only the eight lowest-loss samples. In both cases, the solid line is a least-squares fit to the seven lowest-loss samples, those having less than 0.15 vol % c-axis-oriented grains misaligned at 45°. The dashed line passes through the origin and the average of the two highest-loss samples.

the films which do not correlate well with R_s.

X-ray scans along the majority phase [001] direction show the films are nearly pure c-axis-aligned $YBa_2Cu_3O_7$. It is found that, in some cases, weak impurity peaks appear and in some cases, features which may be indicative of small amounts of a-axis $YBa_2Cu_3O_7$ are found; Fig. 3(a) shows the x-ray data from the sample which had the largest impurity phase peak and Fig. 3(b) shows the c-axis scan from the sample which had the largest feature consistent with a-axis $YBa_2Cu_3O_7$.

Using x-ray techniques, the impurity phase is found to be highly oriented. Transmission electron microscopy (TEM) studies of the sample with the largest impurity peaks reveal that aligned impurities exist as small precipitates at a low volume fraction. A representative micrograph is shown in Fig. 4. A sample which shows no impurity peaks in the c-axis scan was also examined by TEM. No impurity phases are found in the TEM micrographs. X-ray data are used to estimate the relative amounts of impurity phase in each sample, as shown in Table I. Comparison to R_s values shows that changes in impurity phase concentration do not dominate the variations in R_s in these films.

As can be seen from Table I, the appearance of weak features suggesting a-axis $YBa_2Cu_3O_7$ does not correlate to R_s. In a parallel study, it is found that $YBa_2Cu_3O_7$ thin-film samples containing at least 100 times higher volume fraction a-axis grains have losses only four times higher than the lowest-loss samples discussed here.[13] Furthermore, as shown in Sec. V below, those losses can also be accounted for by high-angle grain boundaries amongst c-axis-aligned $YBa_2Cu_3O_7$. Neither such small quantities of impurity precipitates nor such small quantities of a-axis-aligned $YBa_2Cu_3O_7$ contribute appreciably to the residual rf losses observed in these films.

The surface smoothnesses of two films are measured with scanning force microscopy.[14] While their microwave losses differ by a factor of 2.5, they both show a similar rather random pattern of undulations with peak-to-peak variations up to 100 Å and lateral periods close to 2500 Å. A representative scan is shown in Fig. 5.

Rocking-curve widths of the (005) $YBa_2Cu_3O_7$ reflection and c-axis lattice parameters of $YBa_2Cu_3O_7$ appear along with R_s in Table I. These parameters do not correlate with R_s as strongly as the amount of misaligned material. There is no *a priori* reason why either of these parameters should closely follow the volume fraction of c-axis material misaligned in the surface plane. The variations in these features therefore imply that additional structural and microstructural variations are present in these films. It is shown in the next sections that a range of electrical properties, very likely related to a range of microstructures apart from the misaligned c-axis material, is observed for these samples.

IV. CORRELATION OF MICROWAVE LOSS AND dc PROPERTIES

The dc resistivity as a function of temperature is shown in Fig. 6(a) for the lowest-loss film. The normal-state dc resistivity is nearly a linear function of temperature over the range studied and the transition to the superconducting state is sharp. Qualitatively, the data for all but one of the films are similar. The unique sample has a less linear temperature dependence, as can be seen in Fig. 6(b). Overall, there are small variations in the transition widths. Also, the data from different samples differ in the end point of the transition (T_c) and the normal-state resistivity extrapolated to 0 K [$\rho_n(0)$]. These latter two changes are not independent, as shown in Fig. 7. The observed values for $\rho_n(0)$, $\rho_n(100)$, T_c, the superconducting transition widths, and critical currents at 4.2 K appear in Table II. Transition characteristics for the sample which is not patterned are derived from ac susceptibility measurements.

The dc transport data correlate well with R_s among

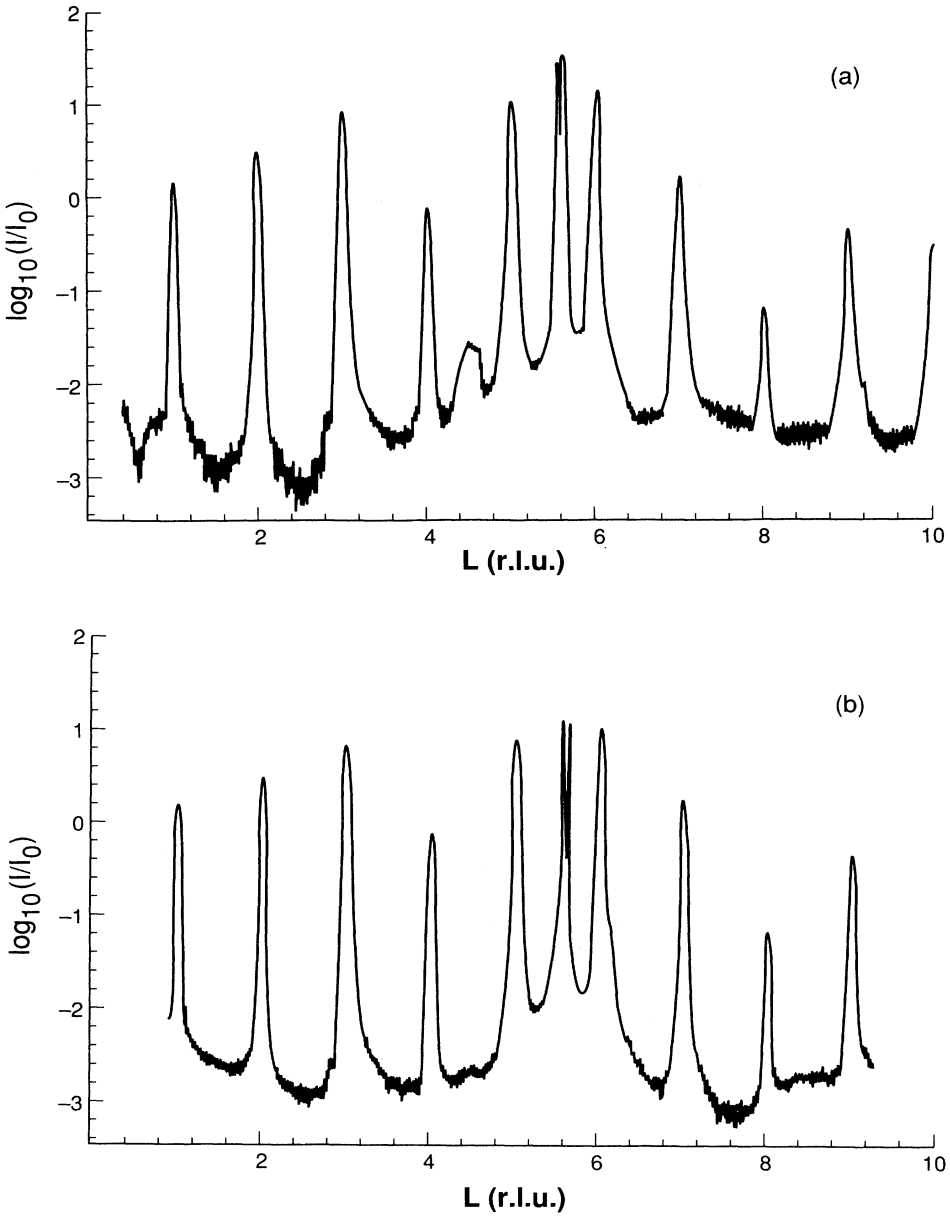

FIG. 3. X-ray-diffraction scan radially along the $YBa_2Cu_3O_7$ c axis from (a) the sample showing the largest impurity reflection ($R_s = 23$ $\mu\Omega$) and (b) the sample showing the strongest indication of possible a-axis-oriented $YBa_2Cu_3O_7$ ($R_s = 38$ $\mu\Omega$). The peaks at integer reciprocal-lattice units are the $YBa_2Cu_3O_7$ (00L) reflections. The peak at $L = 5.6$ is the MgO (200) reflection. In (a), the impurity peak appears at $L = 4.5$. In (b), the possible a-axis feature is the shoulder on the (006) reflection.

the lower-loss samples. As determined by the correlation coefficients from linear least-squares fits to the data from the seven lower-loss samples alone, the changes in the dc transport data correlate to R_s better ($r = 0.9$) than the changes in volume fraction of misaligned material ($r = 0.7$). R_s is plotted as a function of T_c for all the samples in Fig. 8(a) and for the lower-loss samples in Fig. 8(b). R_s is plotted as a function of $\rho_n(0)$ in Fig. 9. The two samples with the highest loss in Fig. 8(a) are the two with the largest fractions of misaligned c-axis grains. Their losses are strongly dominated by mechanisms associated with these grains. When only the lower-loss samples are considered, as in Fig. 8(b), a correlation between R_s and T_c is apparent. In view of Fig. 7, a similar result appears when R_s is plotted as a function of $\rho_n(0)$, as in Fig. 9. Which, if either, characteristic is more directly linked to R_s, or whether all three are coupled by a single underlying phenomenom remains to be seen.

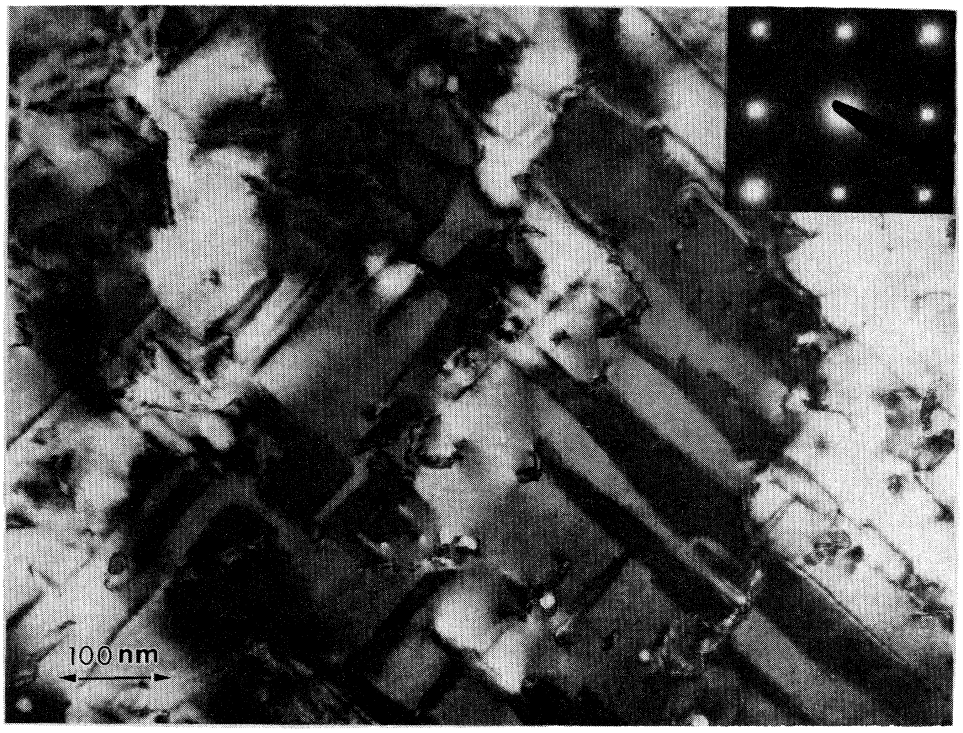

FIG. 4. Transmission electron micrograph in planar view from the sample having the largest impurity reflection in x-ray diffraction and $R_s = 23\ \mu\Omega$.

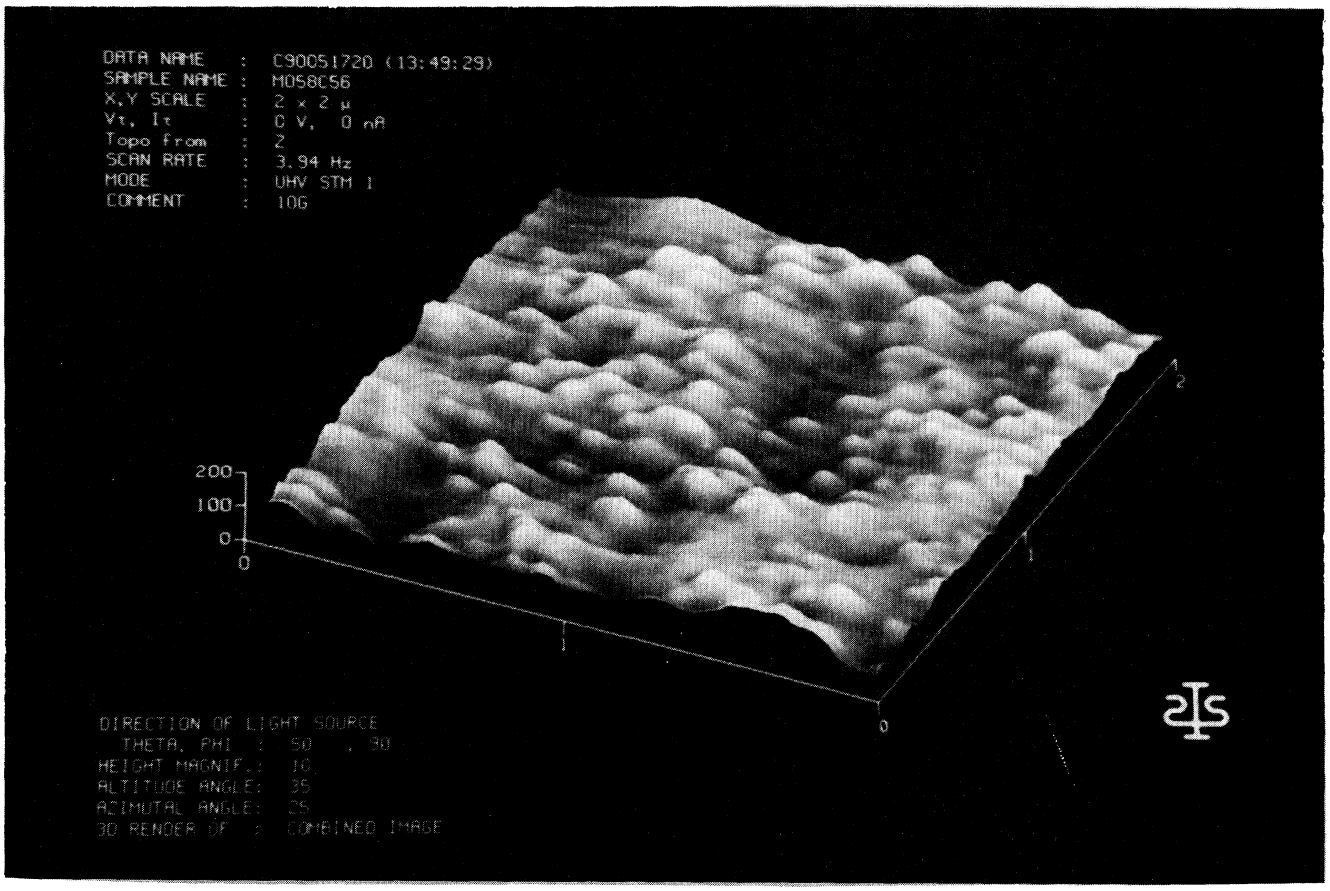

FIG. 5. Scanning force micrograph of the sample having $R_s = 16\ \mu\Omega$.

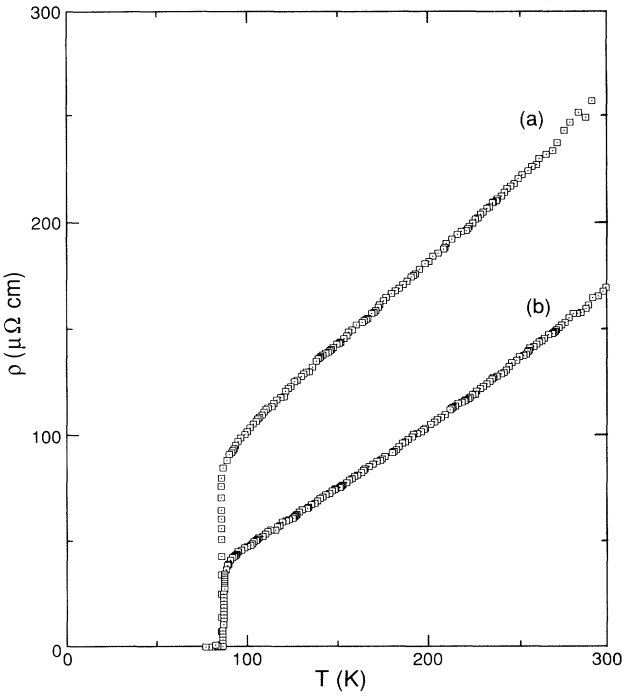

FIG. 6. dc resistivity as a function of temperature for (a) the sample having $R_s = 16$ $\mu\Omega$ and (b) the sample having $R_s = 545$ $\mu\Omega$.

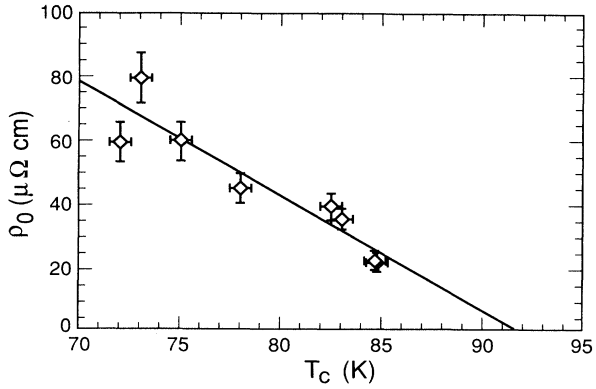

FIG. 7. The correlation between the extrapolated to zero temperature normal-state dc resistivity and T_c. The line is a linear least-squares fit to the data.

Ideal single crystals of $YBa_2Cu_3O_7$ are expected to have lower normal-state resistivities and higher T_c's than shown by the films discussed here. It is thus seen that, with the exception of the film with the highest fraction of misaligned c-axis grains, R_s tends to be higher for the films which deviate more in their dc electrical properties from those expected for ideal single crystals. In this regard, it is worthwhile noting that, unlike the correlation displayed in Fig. 2(b), the trend in Fig. 8(b), and possibly in Fig. 9, appears to extrapolate to R_s values significantly lower than the lowest observed values as lower normal-state dc resistivities and higher T_c's are approached.

The microscopic origin of the differences in dc characteristics is not yet known for these samples. The dc data are not directly attributable to the high-angle grain boundaries. At zero frequency, the influence of such a small number of boundaries on the measured resistivity is expected to be negligible. This expectation is borne out by the sample studied here which has the highest measured fraction of misaligned grains, the lowest normal-state resistivity, and the highest, T_c. The dc behavior does qualitatively correspond to a general depression of the order parameter in the lower T_c samples. On the basis of the process history and previous experience, it is unlikely that the samples are deficient in oxygen in a manner which may be modified by low-temperature oxygen anneals.[3] To be certain this is so, the sample with a loss of 26 $\mu\Omega$ was annealed for 72 h at 450° C. Neither T_c nor R_s changed by more than their uncertainties. The varia-

TABLE II. R_s and dc electrical characteristics (extrapolated to zero-temperature normal-state resistivity, normal-state resistivity at 100 K, superconducting transition temperature, superconducting transition width, and critical current at 4.2 K and 3 kG, respectively) for the $YBa_2Cu_3O_7$ films.

R_s (10 GHz, 4.2 K) ($\mu\Omega$)	$\rho_N(0)$ ($\mu\Omega$ cm)	$\rho_N(100)$ ($\mu\Omega$ cm)	T_c (K)	δT_c (K)	J_c (4.2 K, 3kG) (10^7 A/cm^2)
16	22	100	84.5	1	2
23	35	110	83	1	2
25	21	90	84.5	1	2
26			84	1	
38	45	120	78	2	2
42	39	120	82	1	2
64	60	130	72	3	1
108	60	135	75	3	0.4
545		50	85	2	2
744	80	155	73	3	0.2

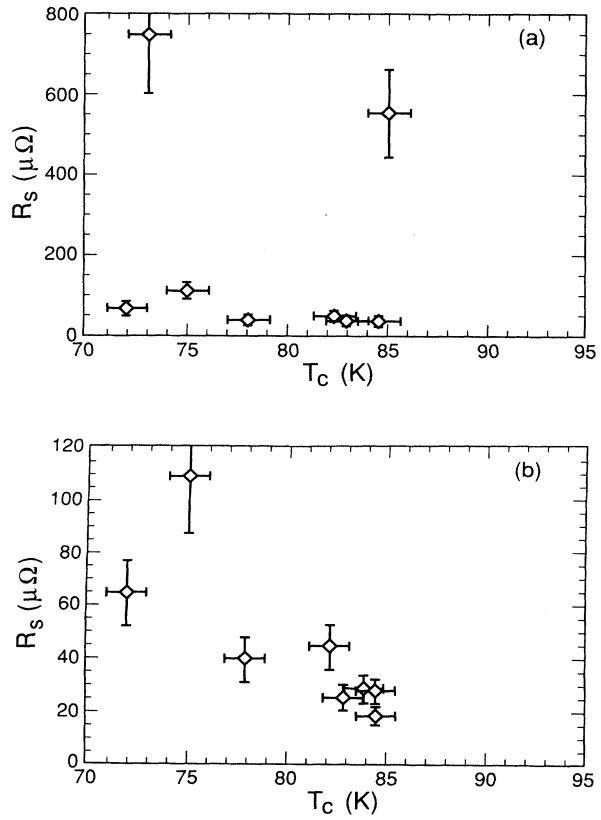

FIG. 8. R_s vs T_c for (a) all samples and (b) the eight lowest-loss samples.

tions in dc properties among the lower-loss films are, however, similar in some respects to the variations found by White *et al.* as a result of low doses of ion irradiation of $YBa_2Cu_3O_7$ thin films.[15] There, the changes in resistivity and persistence of relatively sharp transitions at lowered temperatures is attributed to the creation of damaged regions on the order of 8 Å in diameter which act both to scatter carriers in the normal-state and to lower the amplitude of the pair wave function below the transition, thus depressing T_c. In a related study, small changes in the Hall coefficient as a function of temperature are found for such samples, in the direction which would correspond to a slight drop in carrier density with increasing irradiation.[16] The correspondence of the ion damage results to the study here is obscured by the lower and strongly damage-dependent critical currents and the higher normal-state resistivities observed for all the samples, including the unirradiated samples, in the work of White *et al.* The changes seen here, however, may be microscopically similar and driven by disorder incorporated during the *in-situ*-growth process. Whatever the origin, strong precedents lead to associating the lower T_c's with lower average superconducting condensate density.

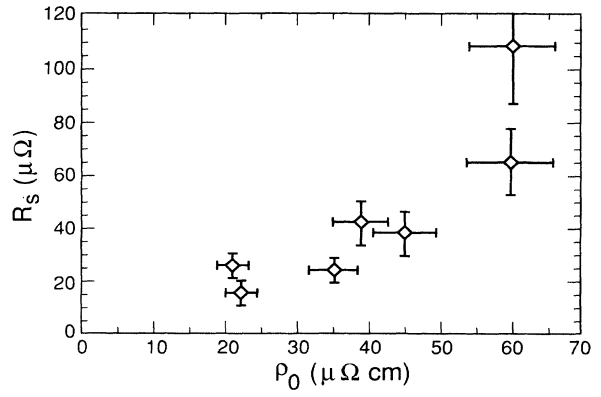

FIG. 9. R_s vs the extrapolated to zero temperature normal-state resistivity for seven of the eight lowest-loss samples. The eighth of the lowest-loss samples was not patterned.

The critical currents for the films at 4.2 K are listed in Table II. They are as high as any reported for $YBa_2Cu_3O_7$ films and approaching estimated depairing currents. Such high critical currents are indicative of high concentrations of defects which may contribute significantly to the measured losses.[17] Seven of the samples which span nearly the full range of observed R_s values all have the same high critical current value at 4.2 K. The field dependencies closely match at fields between 1 and 15 kG. While the defects leading to high critical currents may contribute to the microwave losses in these samples, critical currents, as measured here, do not correlate to *changes* in R_s among these samples.

V. MICROWAVE LOSS MECHANISMS

Some aspects of the data described in this report can be explained quantitatively with existing theories. In this section, the magnitude of the loss in the lowest-loss sample, the lowest loss yet reported for $YBa_2Cu_3O_7$, is placed in the context of conventional expectations and shown to be high. Then, the losses associated with the highly misaligned *c*-axis grains are estimated using a procedure based on an existing microscopic model for microwave losses due to weak links. This model successfully explains the magnitude of the slope of the correlation between R_s and the volume fraction of highly misaligned *c*-axis grains. The contribution of high-angle boundaries to the loss in the lowest-loss sample is then estimated and found to be a small part of the total loss, as is consistent with the empirical trends described in Sec. III. Some possible sources for the remaining loss are then discussed briefly.

The value of the loss in the lowest-loss sample, 16 $\mu\Omega$, is orders of magnitude higher than an intrinsic R_s value from a conventional superconductor at the same reduced temperature, T/T_c. The simplest way to see this is so is to recognize that the measured loss is virtually the same for Nb at 4.2 K. At that temperature, roughly 25% of the carriers in the Nb are uncondensed.[18] Even after accounting for the difference in penetration depths, this corresponds to many more unpaired carriers than Nb would have at the same reduced temperature. We have done more elaborate, although fundamentally equivalent,

comparisons to isotropic BCS-like behavior using the program of Halbritter[19] and parameters roughly appropriate for our $YBa_2Cu_3O_7$ films. For example, taking $T_c=85$ K, the London penetration depth $\lambda_l=1400$ Å, the superconducting coherence length, $\xi_c=20$ Å, a mean free path $l=500$ Å, and gap parameter $2\Delta/kT_c=3.6$, R_s at 4.2 K, is calculated to be more than 10 orders of magnitude below the resolution limit of the apparatus used here. Of course, real superconductors have low-temperatures losses well above their intrinsic levels. For example, high-quality Nb at a very low temperature typically has a loss only 3 orders of magnitude lower than the lowest $YBa_2Cu_3O_7$ loss observed here.[20] Even by this standard, the low-temperature losses in the best $YBa_2Cu_3O_7$ film appear high.

The loss in the lowest-loss sample can be cast in the form of two-fluid parameters. It is shown elsewhere that the lowest-loss film has an experimentally derived penetration depth in the vicinity of 1400–2000 Å.[6] Using the formula[21]

$$\sigma_1=\frac{2R_s}{\omega^2\mu_0^2\lambda^3}\ , \tag{1}$$

where σ_1 is the real part of the complex conductivity, ω is the angular frequency of the microwaves, μ_0 is the permittivity of free space, λ is the penetration depth, and R_s is the surface resistance, then the normal channel conductivity is found to be in the range of 6400–19 000 $(\Omega\,\mathrm{cm})^{-1}$, depending on the exact penetration depth assumed. Models attempting to describe the loss in this film must, when reduced to a two-fluid equivalent, yield a σ_1 in this range.

A detailed examination of R_s in an isotropic BCS model or a two-fluid equivalent circuit indicates that this σ_1 implied by our data cannot be rationalized by a long mean free path. Large effective normal channel carrier densities are required. A very rough estimate of that density can be made utilizing material-specific parameters. If the total carrier density and the mean free path for normal carriers is known, then, in a two-fluid model, a specific R_s value implies a unique fraction of uncondensed carriers. Estimating the total carrier density for $YBa_2Cu_3O_7$ as 1.4×10^{21} cm^{-3} and the mean free path from the extrapolation of the experimentally derived normal-state resistivity, a loss of 16 $\mu\Omega$ corresponds to a normal fraction of 25% and a penetration depth of 1600 Å. Note that the penetration depth is consistent with the experimentally derived estimate for the sample having a 16-$\mu\Omega$ microwave loss. The two-fluid parameters provide an additional perspective on the magnitude of the loss in the lowest-loss sample, showing again that, according to conventional expectations, it is high.

Whether the correspondence of the lowest loss with such a large effective normal fraction is primarily related to extrinsic or intrinsic factors is not yet clear. Higher losses obviously have an extrinsic component. As described in detail next, much, if not all, of the additional losses in the samples discussed in this report can be consistently attributed to the highly misaligned c-axis grains.

The work described in Sec. III makes clear that the losses above the lowest value are correlated in these samples to an increase in the volume fraction of highly misaligned c-axis grains. The appearance of such grains implies the presence of high-angle grain boundaries. Such boundaries show weak-link behavior at zero frequency, fit well by a resistively shunted junction model.[22,23] A quantitative theoretical description of the contribution of weak links to microwave losses appropriate to high-T_c materials is worked out in Hylton *et al.*[4,24] There, the authors systematically examine the effect of one-dimensionally periodic weak-link boundaries, modeled as resistively shunted junctions, on magnetic penetration and resistance as a function of frequency and material parameters. This weak-link model can be used to test the hypothesis that the correlation between R_s and the volume fraction of highly misaligned c-axis grains is directly due to losses associated with those grains' boundaries. To do so, a suitable effective grain size and junction characteristic must be assigned. Since Hylton *et al.* consider a translationally periodic system with a single grain size and single boundary type, a rigorous assignment requires an extension of the model to a nonperiodic inhomogeneous distribution of multiple boundary types in two dimensions. Here we estimate the assignments in simpler way.

We begin by imagining the unrealizable case of 100% misaligned grains. By this we mean the case of a c-axis film made entirely of grains and boundaries which all individually have the characteristics of the real highly misaligned grains and their boundaries in the real films. This case can be analyzed directly with Hylton's formulas. From TEM studies, the misaligned grains in the films studied here are known to have a grain size of about 0.5 μm. From studies by others of similarly prepared films, it is known that the boundaries surrounding such grains may have Josephson critical currents of about 2×10^3 A/cm^2 and I_cR products of 0.2 mV at 4.2 K.[23] The microwave loss at 10 GHz from a semiinfinite sample made up entirely of such grains would be 20 mΩ.

The next step requires estimating to what degree the currents are shunted around the misaligned grains in the real, dilute misaligned boundary case. In general, the exact degree of shunting will depend, in a complicated way, on the detailed characteristics of the grain, the surrounding medium, and the external fields. In view of the good intragrain superconducting properties, to first approximation we ignore the shunting. Then, the contribution to the loss from the high-angle boundaries in the dilute case is estimated by reducing the loss in the 100% case in proportion to the volume fraction of high-angle misaligned grains. (We have in mind that the misaligned grains are as high as the film is thick.) This model agrees well with the experimental results: 3.5% of 20 mΩ is 700 $\mu\Omega$. Quite small densities of high-angle, weak-link boundaries lead to substantial microwave losses. We conclude that the losses in the two highest-loss samples are dominated by this contribution.

Note that highly misaligned c-axis grains are significantly different from insulating impurity phases and a-axis grains. In the case of insulating impurity phases, all current is shunted around the grains. In the

case of *a*-axis-aligned grains, currents may be shunted so that they flow under the grains, in the case that the *a*-axis grains do not extend to the substrate, or so that they flow along the *b*-axis direction. (Microwave current very likely flows much less readily along the *c* axis than along the *b* axis.) Since we know that boundaries between *a*-axis grains aligned at 90° to each other can have critical current densities above 10^6 A/cm^2,[25] it is conceivable that currents passing along the *b* axes between *c*-axis oriented and *a*-axis oriented grains may encounter boundaries with higher J_c's than the boundaries between highly misaligned *c*-axis grains. In the case of highly misaligned *c*-axis grains, current is expected to flow within the grains essentially as well as within the majority of the *c*-axis grains for all directions of current flow within the plane of the film. Also, the entire circumference of such grains' boundaries is a high-angle, weak-link boundary.

Some additional features of the data may also be due to weak-link effects. A wide spread of I_cR products is reported for weak-link, high-angle grain boundaries.[22,23] As R_s is inversely proportional to I_cR in the weak-link model, a spread in R_s values can be expected. We note that considering the losses associated with the samples having close to 0.13 vol % highly misaligned *c*-axis grains alone, the lowest-loss sample and the highest-loss sample have the lowest and the highest normal-state resistivity, respectively. Consistently, the I_cR products of *in-situ*-grown $YBa_2Cu_3O_7$ weak links studied by others are found to be lower in films with higher resistivity and lower T_c's.[22] However, we have so far been unable to match our data to such a model without introducing too many assumptions or parameters for such a small number of data points. Among the complications, the precise value for the penetration depths are not known. Since the decreases in T_c may be due to decreases in condensed carrier densities, as discussed in Sec. IV, and since such decreases would increase the penetration depth, at least this additional source of correlation between R_s and the dc properties should be considered.

As described above, the connection between the high-angle boundary density and microwave loss persists to some degree throughout the series of films studied here. Taken literally, the theoretical calculation just described predicts that only about 5 $\mu\Omega$ ($0.000\,26\times20$ mΩ) out of the measured 16-$\mu\Omega$ loss in the lowest-loss sample can be ascribed to its high-angle grain boundaries. This discrepancy is consistent within experimental error with the empirically derived intercept 12 $\mu\Omega$ shown in Fig. 2(b).

The origin of this remaining component of the loss is not yet known, but a few potential sources of loss can be mentioned. The lowest-loss film is certainly not perfect. We have so far emphasized high-angle grain boundaries, but other boundaries are present. For example, transmission electron microscopy clearly reveals twin boundaries at intervals of 100 nm (Fig. 4). Using the weak-link formulation to treat twin boundary contributions and taking the observed film critical currents as the boundary critical currents, the remaining component of microwave loss would arise from these alone if the boundaries acted as junctions with an I_cR product close to 4 mV. The weak-link formulas are only known to be valid for lower critical currents. Nevertheless, the plausibility of 4 mV as a junction I_cR product is leading us to investigate additional formulations to better test the possibility that twin boundaries contribute significantly to the observed microwave losses. Additional possibilities are suggested by the high critical currents observed for these films. The high critical currents place the films in a class thought to have a very high density of distributed, order-parameter suppressing point defects.[17] For example, if at low temperatures each of these defects is surrounded by a coherence volume of normal metallic material, effective medium calculations show there is a sufficient quantity of normal material to yield the loss level observed here. Variations in such point-defect densities could conceivably also lead to correlations between R_s and the dc properties.[26] These two hypothetical examples, twin boundaries and distributed local defects, underline the possibility that the majority of the microwave loss remaining after taking the high-angle grain boundaries into account is related to extrinsic structural defects. On the other hand, superconducting gap anisotropy is quite possibly an intrinsic feature of $YBa_2Cu_3O_7$. A very low or zero gap value along some directions would lead to a spatially homogeneous density of unpaired carriers much greater than that predicted by isotropic BCS models. With reference to the lowest-loss sample studied here, the quality of $YBa_2Cu_3O_7$ films has improved to the point where such potential intrinsic barriers to lower microwave loss must be considered.

VI. CONCLUSIONS

The lowest resistive loss at 10 GHz and 4.2 K observed for the set of *in-situ*- grown $YBa_2Cu_3O_7$ thin films studied here, 16 ± 3 $\mu\Omega$, sets the lowest accurate upper bound reported to date for the intrinsic loss of $YBa_2Cu_3O_7$. The increase in loss with increasing deviations of the films from the characteristics of ideal, equilibrium single crystals makes clear that values above this level are representative of extrinsic loss mechanisms. It is shown that very small quantities of *c*-axis material misaligned in the surface plane can contribute significant losses. Four percent volume fractions of highly misaligned *c*-axis grains lead to losses above 500 $\mu\Omega$ at 10 GHz and 4.2 K. Our data also show that, for these samples, it is unlikely that the 16-$\mu\Omega$ value is dominated by loss mechanisms associated with the misaligned material. Losses of a different origin dominate. For the lower-loss films in the set, R_s is correlated to the dc transport characteristics. Work continues to attempt to identify the defects responsible for this correlation. The loss level in the lowest-loss film reported here, 16 $\mu\Omega$, implies a real part of its complex conductivity between 6400 and 19 000 $(\Omega\,\mathrm{cm})^{-1}$. This conductivity is consistent with an appreciable density of uncondensed carriers. The study of samples with further improvements in microstructural perfection and normal-state resistivities are desirable for work focusing on the origin of this correspondence.

Note added in proof: We have recently made a similar sample with a measured $R_S = 12\ \mu\Omega$, $x_{45} = 6 \times 10^{-6}$, $T_c = 85$ K, and $\rho_N(100) = 70\ \mu\Omega$ cm. On the scale of Fig. 2(b), these data place the sample at the $x_{45} = 0$ intercept of the solid line.

ACKNOWLEDGMENTS

We thank R. S. Howland, Parks Scientific Instruments, for the scanning force micrograph and K. Char for helpful discussions regarding effective-medium theory. This work was supported in part by the National Science Foundation–Division of Electrical, Communications and Systems Engineering, by the U.S. Air Force Office of Scientific Research, Air Force Systems Command, Department of the Air Force (Washington, D.C.) (AFOSR) under contract No. F49620-88-C-004, by the Center for Research in Superconductivity and Superconducting Electronics under Contract No. F49620-88-C-001, and by the Stanford Center for Materials Research under the National Science Foundation Materials Research Laboratories Program (NSF-MRL) program. T.L.H. acknowledges support from AT&T.

---

*Also at Center for Materials Research, Stanford University, Stanford, CA 94305.

[1]J. P. Turneaure and Ira Weissman, J. Appl. Phys. **39**, 4417 (1968).

[2]M. R. Beasley, Proc. IEEE **77**, 1155 (1989).

[3]C. B. Eom, J. Z. Sun, K. Yamamoto, A. F. Marshall, K. E. Luther, T. H. Geballe, and S. S. Laderman, Appl. Phys. Lett. **55**, 595 (1989).

[4]T. L. Hylton, A. Kapitulnik, M. R. Beasley, John P. Carini, L. Drabeck, and George Gruner, Appl. Phys. Lett. **53**, 1343 (1988).

[5]R. C. Taber, S. S. Laderman, C. B. Eom, and T. H. Geballe (unpublished).

[6]C. B. Eom, J. Z. Sun, S. K. Streiffer, A. F. Marshall, B. M. Lairson, K. Yamamoto, S. M. Anlage, J. C. Bravman, T. H. Geballe, S. S. Laderman, R. C. Taber, and R. D. Jacowitz, Physica C **171**, 351 (1990).

[7]R. C. Taber, Rev. Sci. Instrum. **61**, 2200 (1990).

[8]S. S. Laderman, K. Char, Mark Lee, M. R. Hahn, R. H. Hammond, M. R. Beasley, T. H. Geballe, A. Kapitulnik, and R. Barton, Phys. Rev. B **39**, 11 648 (1989).

[9]C. P. Bean, Phys. Rev. Lett. **8**, 250 (1962).

[10]S. K. Streiffer, B. M. Lairson, C. B. Eom, A. F. Marshall, J. C. Bravman, and T. H. Geballe, Mater. Res. Soc. Symp. Proc. **183**, 363 (1990).

[11]R. Ramesh, D. Hwang, T. S. Ravi, A. Inam, J. B. Barner, L. Nazar, S. W. Chan, C. Y. Chen, B. Dutta, T. Venkatesan, and X. D. Wu, Appl. Phys. Lett. **56**, 2243 (1990).

[12]D. H. Shin, J. Silcox, S. E. Russek, D. K. Lathrop, B. H. Moeckly, and R. A. Buhrman, Appl. Phys. Lett. **57**, 409 (1990).

[13]K. Char, N. Newman, S. M. Garrison, R. W. Barton, R. C. Taber, S. S. Laderman, and R. D. Jacowitz, Appl. Phys. Lett. **57**, 409 (1990).

[14]Parks Scientific Instrument Model SFM-BD2.

[15]Alice E. White, K. T. Short, R. C. Dynes, A. F. J. Levi, Anzlowar, K. W. Baldwin, P. A. Polakos, T. A. Fulton, and L. N. Dunkleberger, Appl. Phys. Lett. **53**, 1010 (1988).

[16]J. M. Valles, Jr., A. E. White, K. T. Short, R. C. Dynes, J. P. Garno, A. F. J. Levi, M. Anzlowar, and K. Baldwin, Phys. Rev. B **39**, 11 599 (1989).

[17]T. L. Hylton and M. R. Beasley, Phys. Rev. B **41**, 11 669 (1990).

[18]Michael Tinkham, *Introduction to Superconductivity* (McGraw-Hill, New York, 1975).

[19]J. Halbritter, Externer Bericht 3/70-6, Institut fur Experimentelle Kernphysik, Karlsruhe (1970).

[20]A. Philipp and J. Halbritter, IEEE Trans. Magn. **MAG-17**, 951 (1981).

[21]T. Dan Duzer and C. W. Turner, *Principles of Superconductive Devices and Circuits* (Elsevier, New York, 1981).

[22]D. Dimos, P. Chaudhari, and J. Mannhart, Phys. Rev. B **41**, 4038 (1990).

[23]S. E. Russek, D. K. Lathrop, B. H. Moeckly, R. A. Buhrman, D. H. Shin, and J. Silcox, Appl. Phys. Lett. **57**, 1155 (1990).

[24]T. L. Hylton and M. R. Beasley, Phys. Rev. B **39**, 9042 (1989).

[25]C. B. Eom, A. F. Marshall, T. H. Geballe, S. S. Laderman, and R. D. Jacowitz, Science **249**, 1549 (1990).

[26]T. L. Hylton and M. R. Beasley (unpublished).

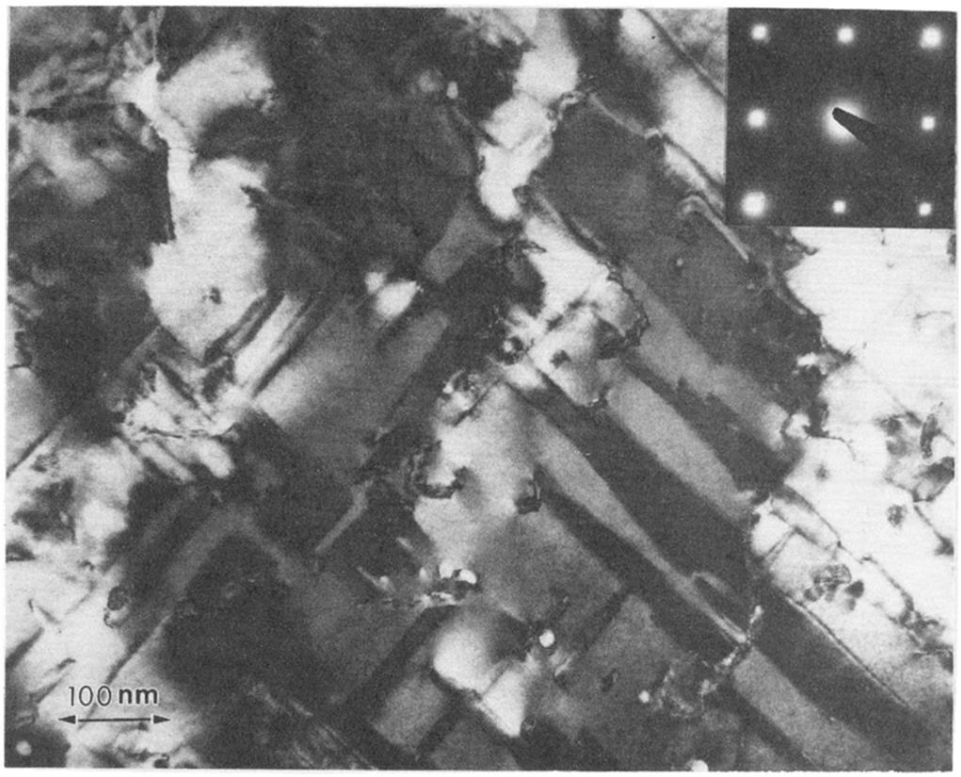

FIG. 4. Transmission electron micrograph in planar view from the sample having the largest impurity reflection in x-ray diffraction and $R_s = 23\ \mu\Omega$.

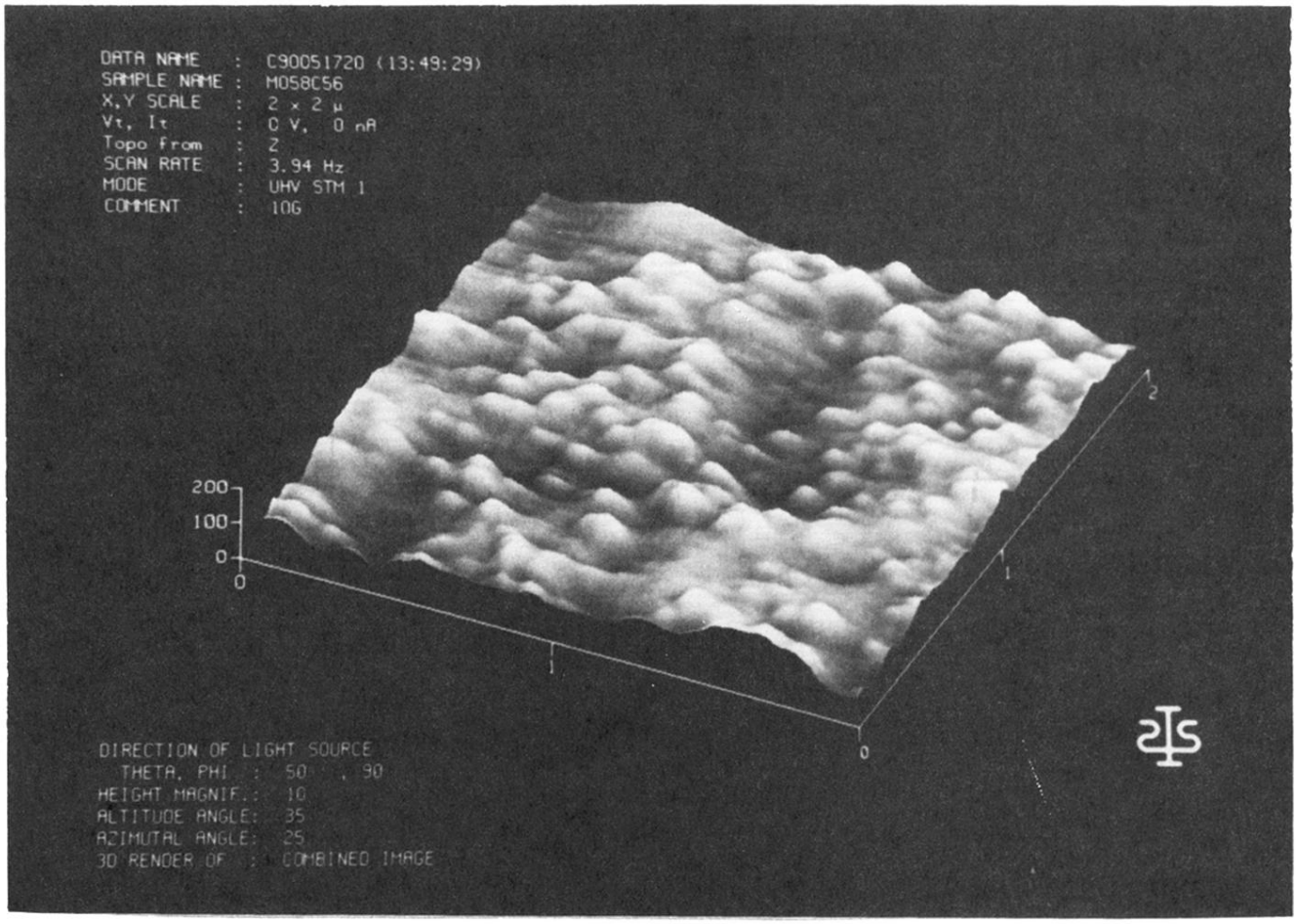

FIG. 5. Scanning force micrograph of the sample having $R_s = 16\ \mu\Omega$.